Proc. of JSCE No. 451/V-17, pp. 255~263, August 1992

A STUDY ON THE APPLICATION OF MODAL PARAMETER IDENTIFICATION USING KALMAN FILTER TO A REINFORCED CONCRETE BRIDGE

Andres W.C. ORETA* and Tada-aki TANABE**

System identification using Kalman filter was applied to an in-situ reinforced concrete bridge to identify its modal properties. A field vibration test was conducted to obtain vibration response data for the purpose of the identification. Using a step-by-step parameter identification technique based on modal analysis of a linear multi-degree of freedom system, the estimation of the modal parameters, which are the dominant natural frequencies and the corresponding damping ratios, was examined. The results from the system identification are presented and compared with those obtained from spectra analysis.

Keywords : *structural dynamics, system identification, Kalman filter, bridge structure, vibration test*

1. INTRODUCTION

The increasing importance of system identification in the area of structural engineering has led to the development and application of various system identification techniques. The growing interest on system identification is motivated by the desire to have a more accurate description of the structure in order to predict its response to external forces, to estimate its existing condition and to assess its degree of damage and deterioration due to severe environmental conditions. One of the system identification techniques that has become increasingly popular in recent years is the Kalman filter.

System identification by Kalman filter has been successfully implemented by many researchers. Hoshiya and Saito[1] solved the identification problems of seismic structural systems using a weighted global iteration technique for stable and convergent solutions. Tanabe and Mizuno[2] identified the structural parameters of a reinforced concrete space frame using the vibration response of laboratory specimens. Hoshiya and Maruyama[3] investigated the identification of the dynamic parameters of a running load and beam system. Maruyama et al[4] developed techniques for the identification of the modal properties of linear multidegree of freedom (MDOF) systems and estimation of the structural parameters of nonlinear single degree of freedom systems. These applications of system identification by Kalman filter, however, involved either numerically simulated data or experimental data obtained using laboratory models. Since testing of in-situ structures remains the most realistic and reliable way of verifying the validity of the identification techniques to real structures, a research on the application to in-situ structures seems imperative.

In this study, system identification using Kalman filter was applied to an in-situ reinforced concrete bridge deck to identify its modal properties. A step-by-step parameter estimation technique[4] based on modal analysis of a linear MDOF system was adopted to estimate the dominant natural frequencies and the corresponding damping ratios. For the purpose of the identification, a field vibration test using impact-induced excitation was carried out to obtain field vibration response data. The behavior of the step-by-step parameter estimation technique as applied to the bridge is examined and the results are presented and compared with those obtained from spectra analysis.

2. MODAL PARAMETER IDENTIFICATION

(1) MODAL ANALYSIS

A very powerful method that can be used to determine the response of a linear MDOF system is the modal analysis. In modal analysis, the response of the system is computed individually for each normal mode and the total response is obtained by the summation of the contribution of the individual modes. The modal equations permit each mode to be represented by an equivalent single DOF system whose dynamic response is obtained independently.

For a linear MDOF system with n DOF under free vibration, the governing equation of motion is

* Graduate Student, Dept. of Civil Engineering., Nagoya Univrsity (Nagoya 464, Japan)
** Member of JSCE, Dr. Eng., Professor, Dept. of Civil Engineering, Nagoya University

generally given by

$$\boldsymbol{M}\ddot{\boldsymbol{Z}}+\boldsymbol{C}\dot{\boldsymbol{Z}}+\boldsymbol{K}\boldsymbol{Z}=\boldsymbol{0}, \cdots\cdots (1)$$

in which $\boldsymbol{M},\boldsymbol{C},\boldsymbol{K}=n\times n$ mass, viscous damping and stiffness matrices, respectively.

Let $\boldsymbol{\Psi}$ and y be the modal matrix and the generalized response vector of the system, respectively. Invoking the orthogonality conditions[5] on the modal matrix $\boldsymbol{\Psi}$ for the mass and stiffness matrices and assuming proportional damping, Eq.(1) can be transformed into a set of uncoupled modal equations in terms of the generalized coordinates with the substitution of $\boldsymbol{Z}=\boldsymbol{\Psi}\boldsymbol{y}$ as follows

$$\ddot{y}_j+2h_j\omega_j\dot{y}_j+\omega_j^2 y_j=0, \cdots\cdots (2)$$

in which h_j and ω_j are the modal damping ratio and natural circular frequency of the j th mode shape. From Eq.(2), we can derive the modal response of the i th displacement as

$$\ddot{u}_{ij}+2h_j\omega_j\dot{u}_{ij}+\omega_j^2 u_{ij}=0, \cdots\cdots (3)$$

where $u_{ij}=\phi_{ij}y_j$ and ϕ_{ij} is the element of $\boldsymbol{\Psi}$ associated with the j th mode and the i th displacement. Hence, u_{ij} is the j th mode contribution to the i th displacement ; and for every i th displacement, we have n-set of equations of the form Eq.(3). The total i th displacement, when the effects of all the modes are taken into account is obtained by superposition as

$$\boldsymbol{Z}_i=u_{i1}+u_{i2}+\cdots+u_{in} \cdots\cdots (4)$$

(2) THE DISCRETE KALMAN FILTER

As a background the Kalman filter will be briefly described. Consider a discrete linear system described by

$$\boldsymbol{X}(k+1)=\boldsymbol{\Phi}(k+1/k)\boldsymbol{X}(k)+\boldsymbol{\Gamma}(k)\boldsymbol{w}(k) \cdots (5)$$

$$\boldsymbol{Y}(k)=\boldsymbol{M}(k)\boldsymbol{X}(k)+\boldsymbol{v}(k) \cdots\cdots (6)$$

where $\boldsymbol{X}(k)$ is an m-dimensional state vector at time $t=k\Delta t$, $\boldsymbol{Y}(k)$ is an r-dimensional observation vector, $\boldsymbol{\Phi}(k+1/k)$ is the non-singular state transition matrix, $\boldsymbol{w}(k)$ is an m-dimensional system noise vector assumed to be a white Gaussian noise with covariance matrix $\boldsymbol{Q}(k)$, $\boldsymbol{\Gamma}(k)$ is the system noise coefficient matrix, $\boldsymbol{M}(k)$ is an $r\times m$ observational matrix and $\boldsymbol{v}(k)$ is the observational noise vector which is assumed white Gaussian noise, independent of $\boldsymbol{X}(k)$, with zero mean and non-zero covariance matrix $\boldsymbol{R}(k)$.

The Kalman filter algorithm is a recursive procedure which starts from an assumption of the initial state vector $\hat{X}(0/0)$ and its error covariance matrix $P(0/0)$. As the observation data $Y(k)$ are processed, the state vector $\hat{X}(k/k)$ and the error covariance matrix $P(k/k)$ are estimated using the following algorithm[6]:

(1) Store the filter state : $\hat{X}(k/k)$ and $P(k/k)$

(2) Compute the predicted state : $\hat{X}(k+1/k)$
$=\Phi(k+1/k)\hat{X}(k/k)$

(3) Compute the predicted error covariance matrix :
$P(k+1/k)=\Phi(k+1/k)P(k/k)\Phi^T(k+1/k)$
$+\Gamma(k)Q(k+1)\Gamma^T(k)$

(4) Compute the Kalman gain matrix :
$K(k+1)=P(k+1/k)M^T(k+1)[M(k+1)$
$P(k+1/k)M^T(k+1)+R(k+1)]^{-1}$

(5) Compute the filtered state by processing the observation $Y(k+1)$:
$\hat{X}(k+1/k+1)=\hat{X}(k+1/k)+K(k+1)$
$[Y(k+1)-M(k+1)$
$\hat{X}(k+1/k)]$

(6) Compute the new (filtered) error covariance matrix :
$P(k+1/k+1)=[I-K(k+1)M(k+1)]$
$P(k+1/k)[I-K(k+1)$
$M(k+1)]^T+K(k+1)$
$R(k+1)K^T(k+1)$

(7) set $k=k+1$ and return to step (1).

(3) STATE AND MEASUREMENT EQUATIONS

To carry out the system identification, the state vector and measurement equations must be properly formulated. Selecting u_{ij}, $\dot{u}_{ij}$ and $\ddot{u}_{ij}$ as the state variables and regarding the modal parameters h_j and ω_j as augmented state variables, the state vector for the j th mode can be defined as

$$X_j=\{x_{1j}x_{2j}x_{3j}x_{4j}x_{5j}\}^T$$
$$=\{u_{ij}\,\dot{u}_{ij}\,\ddot{u}_{ij}h_j\omega_j\}^T. \cdots\cdots (7)$$

Using the linear acceleration method, Eq.(3) can be transformed into a nonlinear discrete state vector equation

$$X_j(k+1)=\begin{Bmatrix} x_{1j}(k+1)\\ x_{2j}(k+1)\\ x_{3j}(k+1)\\ x_{4j}(k+1)\\ x_{5j}(k+1)\end{Bmatrix}$$
$$=\begin{Bmatrix} D_{11}x_{1j}(k)+D_{12}x_{2j}(k)+D_{13}x_{3j}(k)\\ D_{21}x_{1j}(k)+D_{22}x_{2j}(k)+D_{23}x_{3j}(k)\\ D_{31}x_{1j}(k)+D_{32}x_{2j}(k)+D_{33}x_{3j}(k)\\ x_{4j}(k)\\ x_{5j}(k)\end{Bmatrix}$$
$$=g_j(k) \cdots\cdots (8)$$

where,

$D_{11}=1+(\Delta t)^2D_2/6, D_{12}=(\Delta t)(1+(\Delta t)D_3/6),$

$D_{13}=(\Delta t)^2(1+D_4/2)/3,$

$D_{21}=(\Delta t)D_2/2, D_{22}=1+(\Delta t)D_3/2,$

$D_{23}=(\Delta t)(1+D_4)/2$,

$D_{31}=D_2, D_{32}=D_3, D_{33}=D_4$,

with,

$D_1=-(1+(\Delta t)x_{4j}(k)x_{5j}(k)+(\Delta t)^2x_{5j}^2(k)/6)^{-1}$

$D_2=D_1x_{5j}^2(k)$

$D_3=D_1(2x_{4j}(k)x_{5j}(k)+(\Delta t)x_{5j}^2(k))$

and,

$D_4=D_1((\Delta t)x_{4j}(k)x_{5j}(k)+(\Delta t)^2x_{5j}^2(k)/3)$

Considering the first several predominant modes ($l<n$), the state equation of the system becomes

$$X=\begin{Bmatrix}X_1(k+1)\\X_2(k+1)\\\vdots\\X_l(k+1)\end{Bmatrix}=\begin{Bmatrix}g_1(k)\\g_2(k)\\\vdots\\g_l(k)\end{Bmatrix}+\Gamma(k)w(k),\cdots(9)$$

where $w(k)$ is the system noise vector with covariance matrix $Q(k)$ and $\Gamma(k)$ is the coefficient matrix of the system noise.

The measurement or observation equation can be derived by assuming that the acceleration is used as observation. For the j th mode, the resulting measurement equation can be written as

$$Y_j(k)=[0,0,1,0,0]X_j(k)+v(k)\cdots\cdots\cdots\cdots(10)$$

and the corresponding measurement equation when the first predominant modes are considered is given by

$$Y(k)=[0,0,1,0,0,|0,0,1,0,0,|,\cdots]\begin{Bmatrix}X_1(k)\\X_2(k)\\\vdots\\X_l(k)\end{Bmatrix}+v(k),\cdots\cdots\cdots\cdots\cdots\cdots(11)$$

where $v(k)$ is the observational noise vector with covariance matrix $R(k)$

In our present problem, the state vector equation is nonlinear. So to apply the Kalman filter algorithm, an approximation is used by using the linearized form of the state transition matrix whose elements are given by

$$\phi_{ij}(k+1/k)=\frac{\partial g_i(X(k,t))}{\partial X_j}\Big|_{X(k,t)=\hat{X}(k/k)}\cdots\cdots(12)$$

(4) STEP-BY-STEP PARAMETER ESTIMATION

Incorporating Eq.(9) and (11) in the Kalman filter algorithm, the parameters $x_{4j}(=h_j)$ and $x_{5j}(=\omega_j)$ can be estimated using a step by step approach[3),4)] as follows :

1. First, the system is considered as a single DOF and the approximate values of the first modal quantities are obtained. This step is referred to as NM=1 (free) step.

2. The second modal quantities are identified by considering the system to have two DOF. In this case, the first modal quantities obtained in step 1 are used as initial values for the elements of the state vector corresponding to the first mode and the corresponding diagonal elements of the error covariance matrix are set equal to zero. This step is referred to as NM=2 (fixed) step.

3. Using the estimates of the first step and second step as initial values for the first and second modal quantities, respectively, system identification is performed again and new estimates for the first and second modal quantities are obtained. This step is referred to as NM=2 (free) step.

4. Procedures similar to steps 2 and 3 are applied to the third and higher modes, as necessary.

To obtain stable and convergent solutions, the weighted global iteration proposed by Hoshiya and Saito[1)] can be used.

3. FIELD VIBRATION TESTS

(1) TEST BRIDGE

The bridge considered in this study is the Uomi Bridge which is located at Fukui, Japan. It is a three-span multigirder reinforced concrete bridge. In this study, only one of the end spans was tested. This span of the bridge consists of six girders and three intermediate diaphragms supporting a reinforced concrete slab, as shown in **Fig.1**. In the plan layout of the bridge is shown the notation for the nodes which corresponds to the intersection of the girders and diaphragms.

(2) DESCRIPTION OF FIELD VIBRATION TESTS AND DATA ANALYSIS

Strain-guage type accelerometers were installed at the bottom part of the girders at selected nodes. A weight of about 30 kg was dropped from a height of 65 cm on a specific node and the vertical accelerations at the nodes were measured. The impact load was applied when no traffic was present on the bridge. The acceleration data were recorded on magnetic tape using a 14-channel FM analog data recorder. Since the recorder has only 14 channels with one channel reserved for the impact load, then the accelerations at only 13 nodes can be measured at each test. Therefore, the nodes were grouped as shown in **Fig.2**.

In this study, the vibration data of the nodes from both groups obtained from the field tests when the impact load was applied at node 9 were used. The measured data were processed using an AD converter and stored in the computer. Two sets of digitized data using a sampling time of 0.01 s and 0.001 s were stored. A Fast Fourier Transform (FFT) was computed for 1 024 points of each acceleration record using a sampling time of 0.01 s

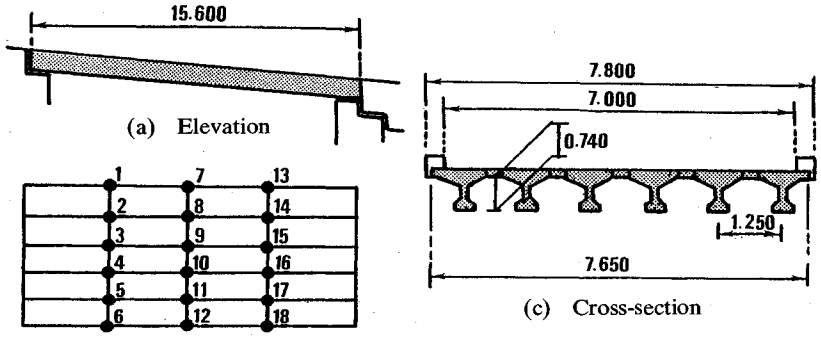

Fig.1 Configuration of Uomi Bridge.

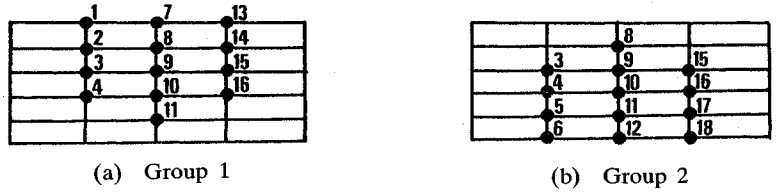

Fig.2 Grouping of Nodes

and the power spectra were obtained. By peak-picking, the natural frequencies were calculated. The corresponding damping ratios were also obtained by using the half-power method. The results of the spectra analysis will be used later for comparison.

Shown in **Fig.3** are the records of the impact load applied at node 9 for group 1 and the resulting vertical acceleration at node 2. **Fig.4** presents the calculated power spectra of some nodes.

4. APPLICATION OF MODAL PARAMETER IDENTIFICATION

(1) APPLICATION OF THE METHOD

The identification procedure was applied to the Uomi Bridge. For each node, the step-by-step parameter estimation approach was carried out to identify the dominant natural circular frequencies and the corresponding damping ratios. For free vibration analysis, the vibration response data (from 1 s to 4 s) after the application of the impact load were used. Using a time increment of 0.001 s, three seconds of the data used for each node corresponded to 3 000 observations. As prior estimates of the state and error covariance matrix are necessary to start the identification, the initial values must be decided. In this study, zero initial values were assumed for both the displacement and velocity. As for the acceleration, the initial value used can be obtained from the recorded data. For the parameters, initial values of 0.1 for the damping ratio h_j, 10.0 or 20.0 for ω_1, 100.0 or 200.0 for ω_2 and 300 for ω_3 were assumed. As for the error covariance matrix, initial values were assumed for the diagonal elements, i.e. 0.01 for the state variables and 100.0 for the parameters. The number of global iteration used was limited to 30 for the first mode identifications and 20 for the higher modes. A weight of 100, which is commonly used, was adopted in the weighted global iteration.

(2) RESULTS OF SYSTEM IDENTIFICATION

The application of the modal parameter identification to the in-situ reinforced concrete bridge using field vibration measurements yielded interesting results. The behavior of the numerical convergence of the modal parameters varied with the node being analyzed. There were nodes where convergent and stable solutions were obtained in the identification of the first modal parameters only. For node 2 of group 1, for example, the identification was succesful for the first two steps of the step-by-step procedure. Using initial values of 0.10 for h_1 and 20.0 for ω_1 and implementing the NM = 1 (free) step, the first modal parameters converged to 0.085258 for h_1 and 59.6004 for ω_1. **Fig.5** shows the convergent behavior of these parameters. It can be seen that after the 8 th global iteration, the parameters become more or less stable as they begin to converge to their final values. For the NM=2 (fixed) step, the state vector was extended to two modes. The values of the first modal parameters obtained previously were fixed and the first estimates of the second modal

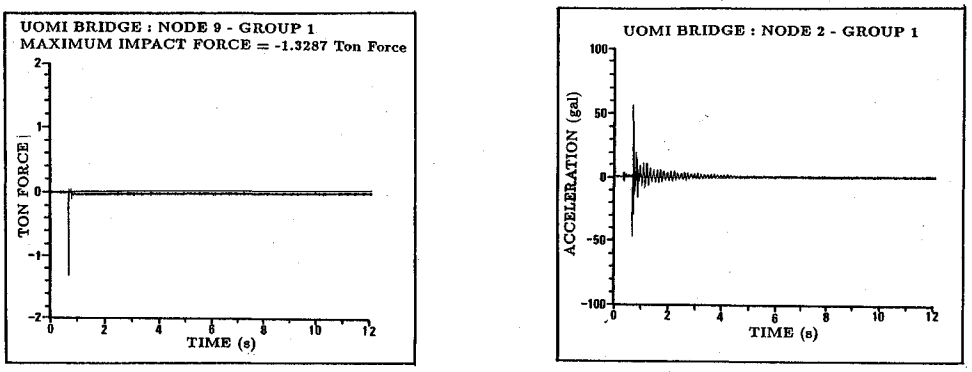

Fig.3 Field Vibration Measurements. (a) Impact Load at Node 9 (Group 1) ; (b) Vertical Acceleration at Node 2 (Group 1)

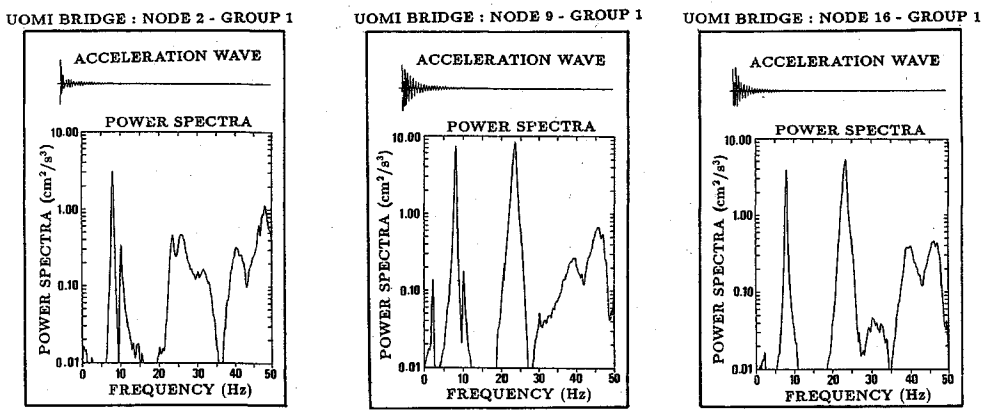

Fig.4 Power Spectra at Selected Nodes of Group 1

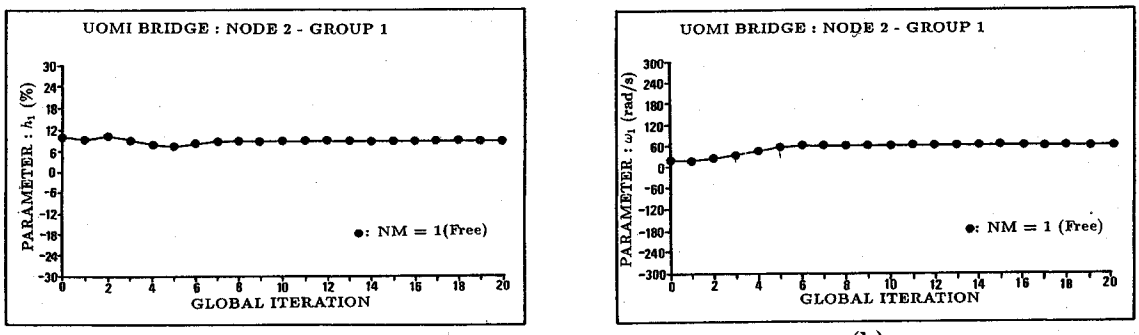

(a) h_1 (b) ω_1

Fig.5 Convergence of Modal Parameters at Node 2 (Group 1).

parameters were calculated. Assuming initial values of 0.1 for h_2 and 200.0 for ω_2, the second modal parameters converged to 0.01141 for h_2 and 84.64 for ω_2. To obtain new estimates of the first and second modal parameters, the NM=2 (free) step was performed wherein the values of the first and second mode estimates were used as initial values. When this step was performed, however, unstable or divergent solutions similar to **Fig.6** resulted. This may be because the second mode response was not appreciably excited as can be seen in Figure 4 where the second and higher frequencies were not well defined for node 2. So the identification was terminated at this step.

For some nodes, convergence was achieved up to the second mode. For node 9 of group 1, for example, the identification was successful up to the NM=2 (free) step. A summary of the step-by-step procedure showing the final values of the parameters at each step at node 9 (group 1) is presented

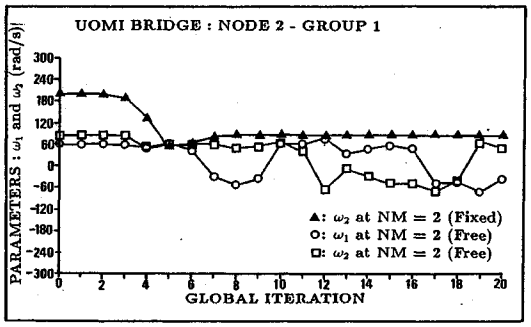

Fig.6 Behavior of ω_1 and ω_2 at Node 2 (Group 1)

in **Table 1.** It is shown that new and improved estimates of the first and second modal parameters were obtained at the NM=2 (free) step.

The behavior of numerical convergence of h_1,ω_1,h_2 and ω_2 at node 9 (group 1) is shown in **Fig.7** (a-d). The convergence of these parameters exhibited a very interesting trend. In the case of ω_1 the first estimate obtained at the NM=1 (free) step converged to a value greater than the estimate at the NM=2 (free) step as shown in **Fig.7** (b). It seems that at the NM=1 (free) step where only one mode was considered, ω_1 tends to be overestimated to compensate for the significant higher modes which were neglected. At the NM=2 (free) step, ω_1 converged to a value less than that at the NM=1 (free) step since the contribution of the higher second mode was now considered. An opposite trend can be observed for ω_2 in **Fig.7** (d). The first estimate at the NM=2 (fixed) step converged to a value less than that at the NM=2 (free) step. This was expected since at the NM=2 (fixed) step, ω_1 was fixed to a value which was greater than that at the NM=2 (free) step. For the case of the damping ratio h_1 the first and second estimates did not vary too much as can be seen in **Fig.7** (a). However for h_2 in **Fig.7** (c), the first estimate at the NM=2 (fixed) step had a negative value and the second estimate converged to a value which was almost similar to h_1.

Extending the identification to 3 modes resulted with the third modal parameters particularly ω_3 converging to values less than the second modal parameters at the NM=3 (fixed) step and divergent solutions at the NM=3 (free) step. This might have been also caused by the third mode response not appreciably excited as can be seen in **Fig.4.** Hence, the identification was terminated at this step.

The identification at a specific node is considered to be successful if convergence reaches the free step. For most of the nodes in this study, the identification was successful only up to the first mode, i.e. convergence did not reach the NM=2 (free) step. It was only for nodes 9, 10, 15, 16 of group 1 and nodes 3, 9, 15 and 16 of group 2 that convergent and stable solutions were obtained up to the NM=2 (free) step. These nodes where convergence reached the second mode were located near the center of the bridge where vibration was expected to be significant.

Table 1 Estimated Parameters for Two-Mode Identification at Node 9 of Group 1 (h_j : damping ratio, ω_j : natural circular frequency in rad/s)

	Initial value	Estimated values		
		NM=1(free)	NM=2(fixed)	NM=2(free)
h_1	0.10	0.036533	–	0.010295
ω_1	20.0	89.3398	–	50.5704
h_2	0.10	–	-0.118966	0.011467
ω_2	100.0	–	122.7250	132.0980

(3) COMPARISON AND DISCUSSION OF RESULTS

The results from the system identification will now be compared with the values obtained from spectra analysis. The estimated natural cyclic frequencies f_j were calculated using the relation $\omega_j = 2 \times \pi \times f_j$.

Tables 2 A and 2 B present the comparison for the nodes where only one-mode identification was successful in group 1 and group 2, respectively. It is shown that the estimated f_1 values at some nodes are quite acceptable and are fairly close to the spectra analysis values with errors less than 10 %. The damping values, however, were poorly estimated.

Tables 3 and 4 present the comparison of results were two-mode identification was successful. **Tables 3** A and 4 A are for the first mode results of group 1 and group 2, respectively ; while **Tables 3** B and 4 B are for the second mode results. The estimates of f_1 for these nodes are better than the estimates obtained from one-mode identification. Here, the errors are less than 4 %. The f_2 estimates are also in close agreement with the spectra analysis values with the errors less than 20 %. The f_1 values were estimated better than the f_2 values. Damping, however was also poorly estimated.

It is interesting to note that the f_1 estimates obtained from the one-mode identification were always greater than the spectra analysis values unlike the f_1 estimates obtained from the two-mode identification. An overestimation seemed to be the trend for the case of one-mode identification. This may be due to the presence of a higher but unidentifiable frequency. An analysis of the power spectra graphs shown in Figure 4 suggests the presence of dominant frequencies in the ranges 5～10 hz and 20～25 hz. Higher frequencies are also visible but they are not well-defined compared to the first two modes. It seems that the modal

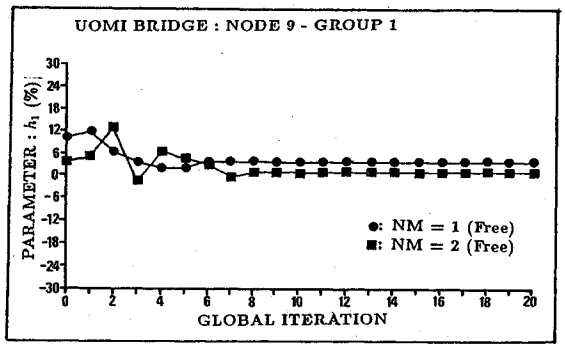

(a) h_1

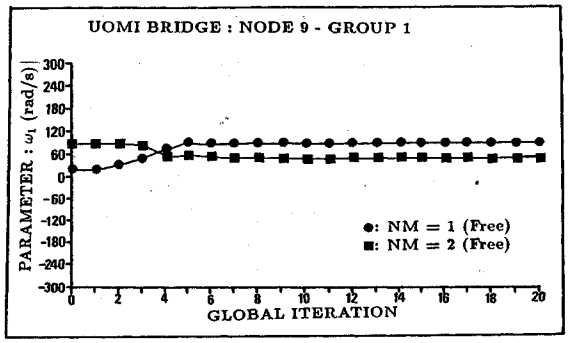

(b) ω_1

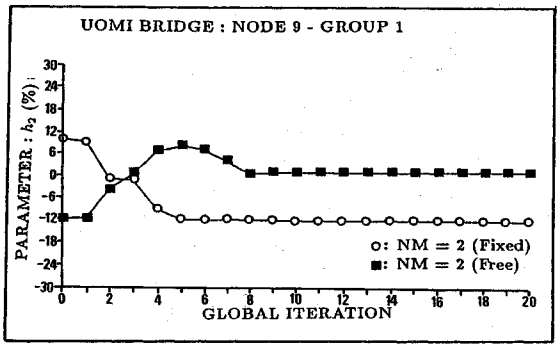

(c) h_2

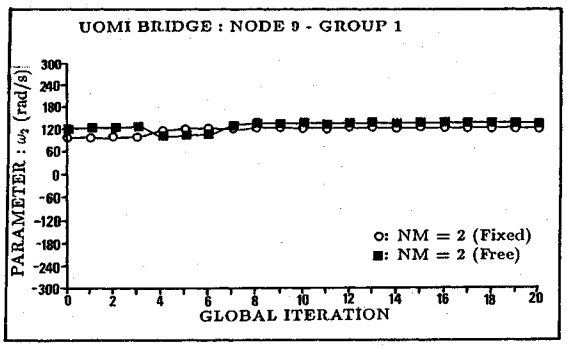

(d) ω_2

Fig.7 Convergence of Modal Parameters at Node 9 (Group 1).

Table 2 A Comparison of Results for Nodes Identified by One-Mode Identification for Group 1 (h_j : damping ratio in percent, f_j : cyclic frequency in Hertz)

Node	h_1(Spec. Anal.)	h_1(Est.)	% Error	f_1(Spec. Anal.)	f_1(Est.)	% Error
1	1.2992	6.5721	-405.86	8.0674	9.4345	-16.94
2	1.3305	8.5258	-540.80	8.0625	9.4857	-17.65
3	1.3156	5.5894	-324.86	8.0879	12.9028	-59.53
4	1.2973	6.4200	-394.87	8.0771	11.6794	-44.60
7	1.2490	2.7355	-119.02	8.0566	11.8995	-47.69
8	1.2899	6.7281	-421.60	8.0625	8.6412	-7.18
11	1.3279	1.3388	-0.82	8.0615	8.0636	-2.60
13	1.3115	4.3061	-228.33	8.0557	10.7034	-32.86
14	1.2704	7.0077	-451.61	8.0576	8.8428	-9.74

Table 2 B Comparison of Results for Nodes Identified by One-Mode Identification for Group 2 (h_j : damping ratio in percent, f_j : cyclic frequency in Hertz)

Node	h_1(Spec. Anal.)	h_1(Est.)	% Error	f_1(Spec. Anal.)	f_1(Est.)	% Error
4	1.4334	6.8073	-374.91	8.0977	11.3889	-40.64
5	1.4131	4.5632	-222.92	8.1016	9.0916	-12.22
6	1.4712	6.9388	-371.64	8.1045	9.8767	-21.87
8	1.4144	3.4769	-145.82	8.0947	8.4392	-4.26
10	1.4045	3.3577	-139.07	8.0947	13.1633	-62.62
11	1.4515	2.9216	-101.28	8.1055	10.5335	-29.94
12	1.4122	2.2222	-57.36	8.1064	10.4939	-29,45
17	1.4140	5.4869	- 288.04	8.0967	10.5344	-30.11
18	1.4517	4.8005	-230.68	8.1044	8.8588	-9.31

Table 3 A Comparison of First Mode Results for Nodes Identified by Two-Mode Identification for Group 1 (h_j : damping ratio in percent, f_j : cyclic frequency in Hertz)

Node	h_1(Spec. Anal.)	h_1(Est.)	% Error	f_1(Spec. Anal.)	f_1(Est.)	% Error
9	1.3325	1.0295	22.74	8.0518	8.0486	0.04
10	1.3206	4.6610	-252.94	8.0615	7.8829	2.22
15	1.1289	3.3981	-201.01	8.0752	7.9478	1.58
16	1.2994	3.6355	-179.78	8.0664	7.9425	1.54

Table 3 B Comparison of Second Mode Results for Nodes Identified by Two-Mode Identification for Group 1 (h_j : damping ratio in percent, f_j : cyclic frequency in Hertz)

Node	h_2(Spec. Anal.)	h_2(Est.)	% Error	f_2(Spec. Anal.)	f_2(Est.)	% Error
9	1.9342	1.1467	40.71	23.4189	21.0240	10.23
10	1.9157	4.8230	-151.76	23.4140	21.2790	9.12
15	1.8688	3.2646	-74.69	23.4499	18.9978	18.99
16	1.9000	2.5414	-33.76	23.4297	19.6644	16.07

Table 4 A Comparison of First Mode Results for Nodes Identified by Two-Mode Identification for Group 2 (h_j : damping ratio in percent, f_j : cyclic frequency in Hertz)

Node	h_1(Spec. Anal.)	h_1(Est.)	% Error	f_1(Spec. Anal.)	f_1(Est.)	% Error
3	1.4532	1.4348	1.27	8.0967	8.0869	0.12
9	1.3649	1.5648	-14.64	8.0947	8.0989	-0.05
15	1.3941	3.9454	-183.01	8.0977	8.0016	1.19
16	1.4134	6.5673	-364.63	8.0996	7.8422	3.18

Table 4 B Comparison of Second Mode Results for Nodes Identified by Two-Mode Identification for Group 2 (h_j : damping ratio in percent, f_j : cyclic frequency in Hertz)

Node	h_2(Spec. Anal.)	h_2(Est.)	% Error	f_2(Spec. Anal.)	f_2(Est.)	% Error
3	1.9207	1.7181	10.55	23.3754	20.1843	13.65
9	1.8668	1.9606	-5.02	23.3691	23.3698	-0.03
15	1.8803	4.6026	-144.78	23.3799	20.6523	11.67
16	1.8107	7.0302	-288.26	23.3760	20.5848	11.94

parameters converged only up to the most significant modes. The first two mode shapes corresponding to the identified frequencies which were obtained by spectra analysis are shown in **Fig.8**. The fundamental frequency for this simply supported bridge corresponds to a vertical mode (**Fig.8** a), while the second lowest frequency corresponds to a torsional mode (**Fig.8** b).

5. CONCLUSION

System identification using Kalman filter was applied to an in-situ reinforced concrete bridge. In the study, vertical acceleration data obtained from field vibration tests were used to identify the modal parameters of the bridge. The results of the identification of modal parameters by Kalman filter were very encouraging. Estimates of the dominant natural frequencies by system identification were close to that obtained by spectra analysis especially when the corresponding mode is appreciably excited. Damping, however, was poorly estimated. This may be due to the assumption of proportional damping which may not be true for this bridge. A more comprehensive research must be conducted to study the effects of sampling time, sampling length, initial values and observational noise on the results of the system identification. With an in-depth study, the consistency of the results can be verified. It is also recommended that vibration data where higher modes are excited be used in future studies.

ACKNOWLEDGMENT

The valuable assistance of Asst. Prof. Masafumi Kato and his laboratory staff during the field vibration tests is deeply appreciated. The support and cooperation of the staff and students of the concrete laboratory of Nagoya University is also appreciated.

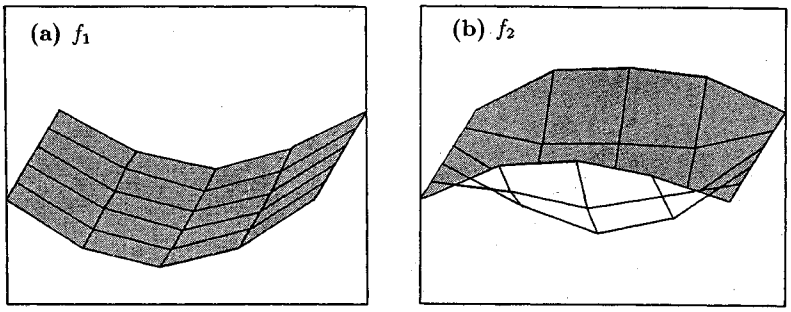

Fig.8 Mode Shapes Corresponding to the First Two Frequencies

REFERENCES

1) Hoshiya, M. and Saito, E. : Structural Identification by Extended Kalman Filter, Journal of Engineering Mechanics, ASCE, Vol.110, No.12, December, pp.1757~1770, 1984.
2) Tanabe, T. and Mizuno, T. : Study on the Identification of Dynamic Response Parameters of RC Structures, Proc. Int. Conf. on Highrise Buildings, pp.499~504, 1989.
3) Hoshiya, M. and Maruyama, O. : Identification of Running Load and Beam System, Journal of Engineering Mechanics, ASCE, Vol.113, No.6, June, pp.813~824, 1987.
4) Maruyama, O., Yun, C.B., Hoshiya, M. and Shinozuka, M. : Program EXKAL 2 for Identification of Structural Dynamic Systems, NCEER Technical Rcport, No.NCEER 89-0014, May, 19, 1989.
5) Barbat, A.H. and Canet, J.M. Structural Response Computations in Earthquake Engineering, Pineridge Press, Swansea, UK, 1989.
6) Jazwinski, A.H. : Stochastic Processes and Filtering Theory, Academic Press, NY, 1970.
7) Oreta, A.W.C. : A Study on the Identification of Dynamic Characteristics of a Reinforced Concrete Bridge by Kalman Filter Theory, Thesis submitted to the Department of Civil Engineering, Nagoya University in partial fullfillment of the requirements for the degree of Master of Engineering, March, 1991.

(Received June 18, 1991)

カルマンフィルター理論によるRC橋のモーダルパラメーター同定に関する研究

Andres W. C. ORETA and Tada-aki TANABE

本研究は，カルマンフィルター理論を用いたシステム同定法を適用し，即存橋梁の動的特性評価を行ったものである．

線形MDOFシステムのモード解析により，現場振動試験で得られた振動特性から，支配的な固有振動数および対応する減衰係数の同定を行った．その結果は，スペクトル解析によるものと比較している．また，モーダルパラメーターの数値収束性についての考察も行った．